

# **The Wheat from the Chaff: Separation of Species in the Exhaust of the Princeton Field Reversed Configuration Fusion Reactor**

*Joseph Abbate, Meagan Yeh*

*Advisors: Samuel Cohen, Bruce Koel*

The Princeton Field-Reversed Configuration (PFRC) concept relies on low-neutron production by D-3He fusion to enable small, safe, nuclear-fusion reactors to be built, an approach requiring rapid and efficient extraction of fusion ash and energy produced by D-3He fusion reactions. The ash exhaust stream would contain energetic (0.1-1 MeV) protons, T, 3He, and 4He ions and nearly  $1e5$  cooler (ca. 100 eV) D ions. The T extracted from the reactor would be a valuable fusion product in that it decays into 3He, which could be used as fuel. If the T were not extracted it would be troublesome because of neutron production by the D-T reaction. This paper discusses methods to separate the various species in a PFRC reactor's exhaust stream. First, we discuss using the electric and magnetic fields of magnetohydrodynamic power generation, direct energy conversion, and curved magnetic fields as plausible frameworks for separating the energetic from the cool components. Then we discuss exploiting material properties such as reflection, sputtering threshold, and permeability, to allow separation of the deuterons from the fast fusion products. In either case, the fast fusion products still need to be separated by species. In our final section, we detail methods of separating the fast fusion products from one another through refrigeration, including a cost analysis.

## Introduction

Nuclear fusion reactors, once successfully operated, have the potential to supply essentially limitless energy. One such reactor is the Princeton Field Reversed Configuration (PFRC). Successfully operating the PFRC requires overcoming many challenges, including the separation of ions exiting the PFRC via the exhaust stream. The exhaust stream is composed of 99.99% deuterons at a couple hundred electron volts, and .01% fast fusion products (tritium, protons, helium 3, and helium 4) at a couple hundred kiloelectron volts<sup>1</sup>. (For purposes of this paper, we largely quantify the deuterons at approximately 200 eV and the fusion products at approximately 200 keV). More specifically, our machine has a flow of order of  $10^{18}$  fusion products / s and  $10^{22}$  deuterons / s per MW of power produced by the reactor. Removing and isolating the tritium is critically important to clean fusion because of its radioactivity and tendency to react with deuterium to form damaging neutrons. Helium 3 is the main source of energy for the PFRC, and deuterium is not only a fuel source but also a coolant. Clearly, the isolation of each of these species is crucial to a sustainable long term fusion reactor.

Due to the vast difference in energies between the 200 eV deuterons and 200 keV fusion products, various methods for separation by energy have arisen in two categories: plasma effects and surface and volume effects. Plasma effects enable the separation by energy to occur before any plasma-wall interactions, thereby allowing different surfaces to be chosen for the

different energy particles. Surface and volume effects, by contrast, rely on the properties of surfaces - reflection, sputtering, and permeability - to separate out the slower deuterons.

Following a separation by energy, the fusion products are separated from the deuterium. However, the fusion products - tritium, hydrogen, helium 3, and helium 4 - still need to be separated from one another. Exploiting the different temperatures of liquefaction of the various species and the superfluid properties of helium 4, refrigeration could be used for this second separation technique. This technique requires extreme cooling, so a cost analysis must be undertaken to determine its feasibility in practice.

## Plasma Effect Separation

### Separation via MHD Power Generation

For many, the first thought to come to mind when considering how to separate charged particles is to use the technique of a mass spectrometer - particles with different masses, charges, or velocities have different gyroradii in the presence of a constant magnetic field running in a direction perpendicular to the velocity. Magnetohydrodynamic (MHD) power generation applies this principle to harvest energy from a fast moving plasma-seeded gas. As shown in Figure 1, a magnetic field in the z-direction causes positive ions to bend to one side and electrons to bend to the other as the gas is expanded; thus, converting flow energy into electrical potential energy<sup>2</sup>. Since the gyroradius is directly proportional to velocity, one could imagine harvesting the higher energy ions (helium 3, helium 4, protons, tritium) from the panels further down the expander and the lower energy ions (deuterium) from the panels close to the entrance.

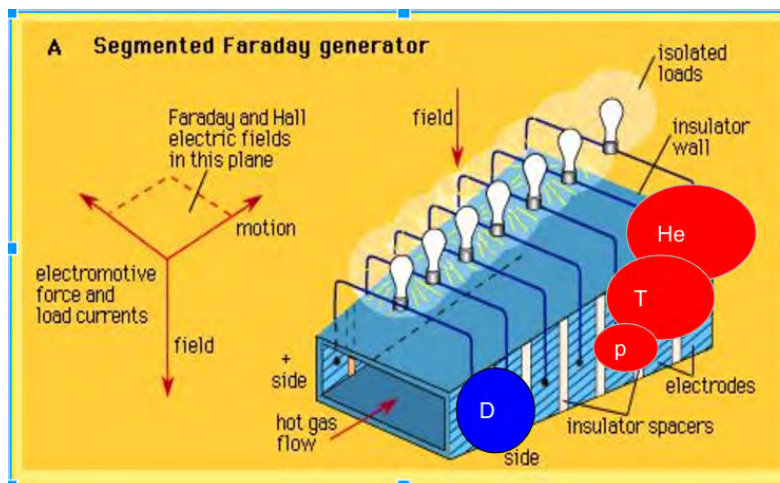


**Figure 1**<sup>2</sup> - A simple, hypothetical schematic of an MHD generator with the PFRC exhaust stream as input also depicting the final positions of the fast fusion products and slow deuterons

### Separation via DEC

Direct energy conversion (DEC) is another method of generating power from a fast flowing plasma. With this method, as depicted in Figure 2, a fast moving plasma's electrons are

reflected by a very low potential and collected at the entrance. Then the positively charged plasma moves through a series of plates of increasing potential, gradually decelerating each individual ion until the ion stops and veers into the plate whose potential corresponds to that ion's initial kinetic energy. In this way, a potential difference is generated between the ions stopped on the plates and the electrons collected at the entrance<sup>3</sup>. This energy can then be stored. Similar to MHD, the idea behind species separation for the PFRC would be to collect the higher energy ions from the higher potential plates and the low energy deuterons from the lower energy plates.

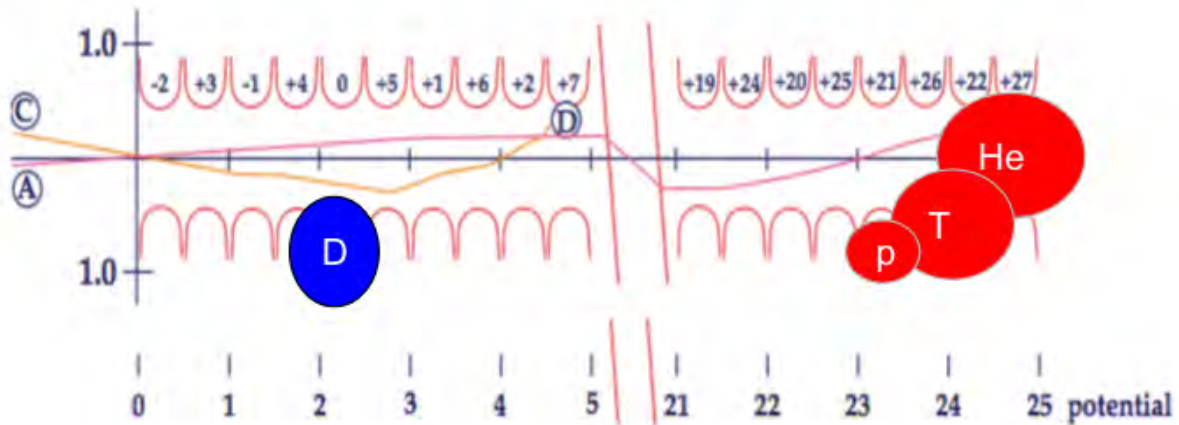


**Figure 2**<sup>3</sup>- Schematic of a DEC with the hypothetical final positions of the slow deuterons and fast fusion products were we to input the PFRC exhaust.

### Analysis of MHD and DEC for the PFRC

Both of these methods would be highly desirable, as they not only separate the fast from the slow species but also allow us to recover kinetic energy rather than let it go to waste as heat. However, there is a fundamental difference between the PFRC's plasma and the plasmas used in MHD and DEC experiments. Our plasma has a very high density (order of  $10^{12}$  particles per cc), and knowing that our electron temperature is 20 eV, the equation

$$\text{Debye Length} = \lambda_D = \left( \frac{kT}{4\pi n e^2} \right)^{\frac{1}{2}} = 7.43 \times 10^2 T^{1/2} n^{-1/2} \text{cm}$$

tells us that our debye length is order of  $10^{-3}$  cm. This is far too small for electric or magnetic fields to be penetrating our plasma as it flows by. For this reason, for either MHD or DEC methods of separation to be feasible, we would have to make our plasma far more tenuous via expansion, as described by Post in a paper on DEC. However, the expander would be order of 10s or possibly even 100's of meters in length<sup>4</sup>. One of the greatest strengths of the PFRC is its small size, which in turn means lower cost and faster construction. A large expander should therefore be avoided if possible, so for now we have put on hold our studies of separation through MHD or DEC methods.

### Curvature Drift Separation

Another potential method for separation could come from the difference in curvature drift due to differences in energy for the fast versus slow products, as demonstrated by the equation

$$\text{Curvature Drift} = \frac{m \mathbf{R}_c \times \mathbf{B}}{q R_c^2 B^2} \left( v_{\parallel}^2 + \frac{1}{2} v_{\perp}^2 \right)$$

Of course, because of the charge dependence we also have a separation of negative electrons from positive ions, which in turn creates an electric field. H.P. Eubank of the Princeton Plasma Physics Laboratory extensively studied these effects for a plasma of the same high order of density (up to  $10^{12}$  per cc) as in the PFRC as it maneuvered through a curved magnetic field. He found that when a plasma, with equi-energetic ions, consisting of hydrogen and impurities (defined as ions whose  $m/Z$  values are greater than that of hydrogen), moved through a curved magnetic field, the higher velocity (lower mass) ions followed the field lines while the lower velocity (high mass) ions ignored the curved field lines and blasted straight on through (see Figure 3)<sup>7</sup>.

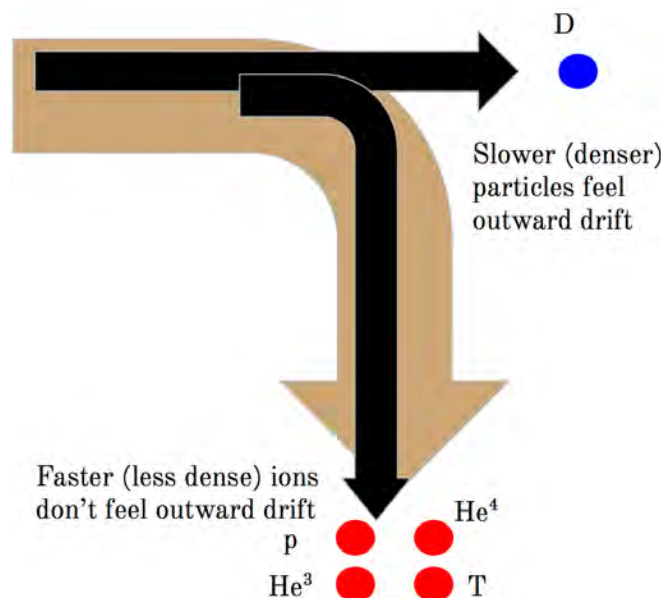


**Figure 3** - Simple depiction of what, based on a *naive* interpretation of Eubank's experiments, would happen to our slow deuterons and fast fusion products when the PFRC exhaust is sent through a curved magnetic field.

George Schmidt of Stevens Institute of Technology was able to put this on a theoretical backing, attributing the straight trajectory of slow ions to the fact that for an ion gun with a single blob of plasma rather than a continuous flow, faster ions comprise a section of plasma of lower density and slower ions comprise a section of higher density (see Figure 4-A). The idea is that the

higher the plasma density, the more significant the electric field generated by the curvature drift separation of electrons and ions in the z direction. This electric field causes an E cross B drift,

$$v_{\perp drift} = \frac{\mathbf{E} \times \mathbf{B}}{B^2} \quad 6$$

which implies a radial force exactly enough to counter the centripetal force necessary to keep ions following the magnetic field lines through the curve<sup>8</sup>. In his aforementioned paper, Eubank confirmed experimentally that the electric field generated by the curvature drift was indeed the culprit. When he increased the conductivity at the gun, shorting out the curvature electric field, more ions followed the curve; thus, enforcing this hypothesis.

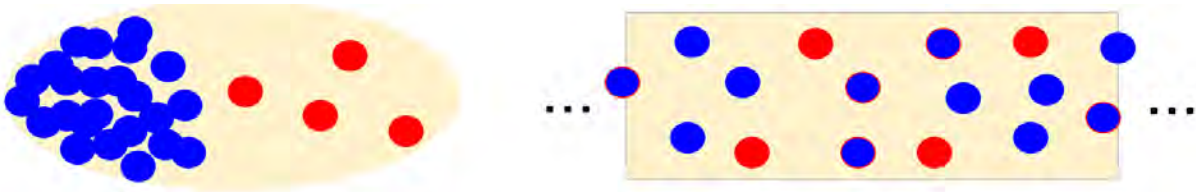


**Figure 4** - Demonstration of the difference between Eubank's and the PFRC's plasmas.

- A. (left)** Eubank's plasma was from a gun that fires a blob of plasma, so that fast ions (red) are part of a tenuous plasma while slow ions (blue) are part of a denser plasma.
- B. (right)** The PFRC plasma is a homogeneous and steadily flowing mixture rather than a blob, where fast and slow ions are in a plasma of a single density.

#### A Novel Separation Approach via Curved Magnetic Field Lines

Of course, the *purification* (removing impurities as previously defined) that Eubank found is of no use to us since we have a continuously flowing, homogeneous plasma rather than a plasma blob (see Figure 4). However, Eubank's conclusions are still extremely useful for us: we now know that our very dense plasma will not obediently follow magnetic field lines around a curve unless we can short out the electric field caused by the curvature drift. With this in mind, Sam Cohen, also of the Princeton Plasma Physics Laboratory, has suggested separating slow deuterons from fast fusion products based on the Larmor radii of fast particles being much smaller than that of the deuterons. This means faster particles will be more likely to disregard a changing magnetic field and barrel through while slower particles would follow the field lines. The idea is to have magnetic field lines expand outward so that deuterium ions follow the lines and become a hollow tube while the fast fusion products retain their cylindrical shape and continue straight (see Figure 5). The key to the idea is that since the expansion is axially symmetric, the curvature drifts of each of the deuterons is in the same orientation of the theta direction. Thus, deuterium ions are *circulated* without developing an electric field. Thanks to this design, we ensure that the deuterons continue to follow the curved field lines despite the high density of our plasma. We highly recommend further studies on this design.

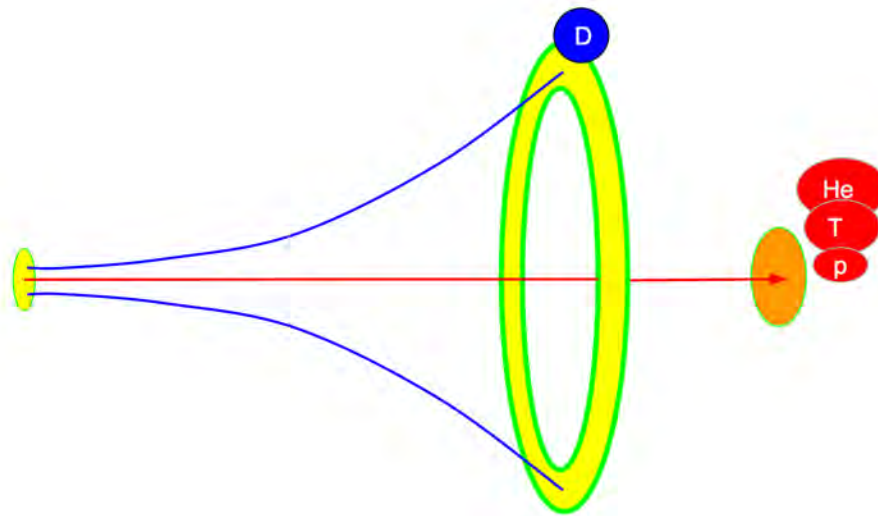


**Figure 5** - Novel idea for separation of slow deuterons from fast fusion products: magnetic field lines (blue) expand outward from the exhaust nozzle (leftmost yellow circle) and deuterons with their small larmor radii follow them to be collected on the yellow annulus (middle) while fusion products with their large larmor radii continue straight on to be collected on the orange plate (right). Note that curvature drift of deuterons merely causes circulation (in the shape of an annulus) thus preventing generation of any electric field.

## Surface Separation

If separation of fast from slow species indeed proves possible, then different surfaces could be utilized to handle the cold deuterons and the hot fusion products. However, if this is not the case, one surface must be adequate for them all. Moreover, this surface must have characteristics of reflection, sputtering, stopping power, and diffusion that allow a separation by energy to be achieved.

### An Overview of Surface Separation

The schematics shown in Figure 6 depict two possible arrangements of surfaces that could produce this separation. In Figure 6-A, a first surface acts as the material all ions originally come in contact with. The slow deuterons will either reflect back or stop almost instantaneously within the first surface. Then they will diffuse back out from the surface because the diffusion barrier will prohibit diffusion into the fast ion stopping material. The fusion products, on the other hand, will have enough energy to blast through both the first surface as well as the diffusion barrier and will then become implanted in the fast ion stopping material. Again, the diffusion barrier will prohibit diffusion back into the first surface. Thus, the fusion products will diffuse out the fast ion stopping material and the species will be sorted based on energy. Figure 6-B represents a similar idea. The only difference is the omission of the first surface. Instead, the diffusion barrier will act as a first surface, allowing the fusion products to have more energy to continue through a thicker diffusion barrier because they won't be slowed down by an alternate first surface. The deuterons will instead be either reflected off or implanted into the diffusion

barrier, but due to their low energy, they will stop very close to the surface. Thus, they will most likely diffuse out the diffusion barrier instead of continuing into the fast ion stopping material. The fusion products behave the same as they do in the previous schematic once implanted in the fast ion stopping material. We will discuss the efficacy of each later in this section.

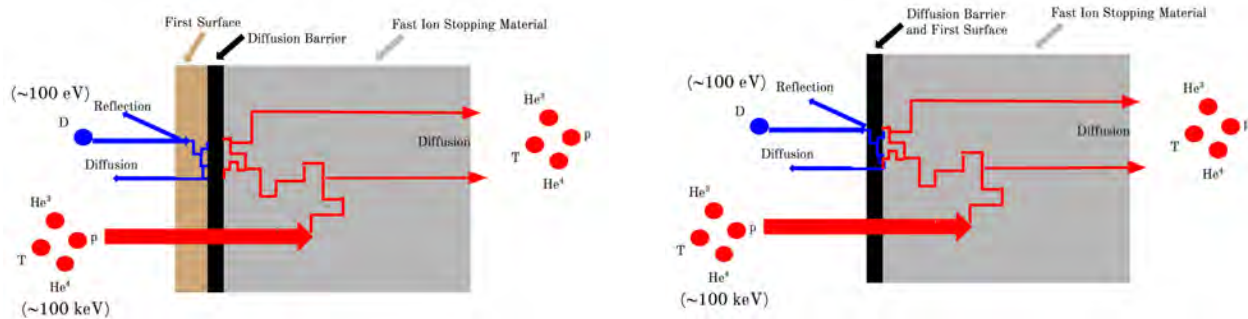


**Figure 6** - Two potential designs for the separation surface.

- A. (left)** A primary surface (brown) reflects deuterons, a diffusion barrier (black) insures that deuterons that do go through ultimately are reflected back to the left, and the fast products blast through both to be stopped in the tertiary material (silver).
- B. (right)** The diffusion barrier also acts as the primary surface that reflects most of the deuterons.

In either schematic, one of the main properties the first surface must achieve is a sputtering energy threshold above the energy of the 200 eV deuterons that comprise the bulk (~99.99%) of the flux hitting it. This will eliminate the main source of sputtering, and allow the material to last for an appropriate amount of time. Thus, it was reasonable to consider tantalum (sputtering energy threshold ~ 315 eV) as a material for our first wall in Figure 6-A<sup>8</sup>. Additionally, tantalum pentoxide was considered for our diffusion barrier, as it would also make a good diffusion barrier and first surface in Figure 6-B with sputtering energy threshold 250 eV for deuterium ions<sup>9</sup>. Furthermore, oxygen ion implantation could potentially allow one continuous block of tantalum to be injected with oxygen to create the tantalum pentoxide diffusion barrier a designated distance away from the surface. This ease of manufacturing makes this combination of first surface and diffusion barrier particularly attractive, but further research on this method is required.

After identifying the appropriate materials to be either tantalum or tantalum pentoxide, the optimal thicknesses of the first surface and diffusion barrier need to be determined. If the surfaces are too thick, the fast fusion products will not be able to clear them and the separation will not succeed. On the other hand, if the material is too thin, it will be sputtered away quickly and will require more maintenance.

### Stopping Power and Maximal Thickness

To identify the *thickest* the wall can be, we examine the stopping power, or energy lost by a particular ion upon crossing a single monolayer of a particular surface. With stopping power graphs (as a function of energy) compiled by Helmut Paul of the International Atomic Energy

Agency, we integrate the inverse of the stopping power between the final and initial energy to get the amount of energy the ion retains as a function of the distance it has passed through the surface<sup>10</sup>. The graphs of these variables for helium on tantalum with impacting ion energies of 200 and 500 keV are shown in Figure 7. Note that we carry out the integration by approximating the functions within the range in question to be of the form  $ax^b$ , where b and a can be easily determined by choosing two points on the graph (see Figure 8 for an example of what the graphs look like). It not only turns out to be fairly accurate for all the values along the way, but also captures the fact that stopping power must of course go to 0 as energy approaches 0, which is the reason for the very physically significant up-flip of the depicted graphs near 0 energy. Also, note that we use helium 4 for our calculations since it is our worst case scenario, since it stops the quickest because it has the highest mass of all of the fusion products.

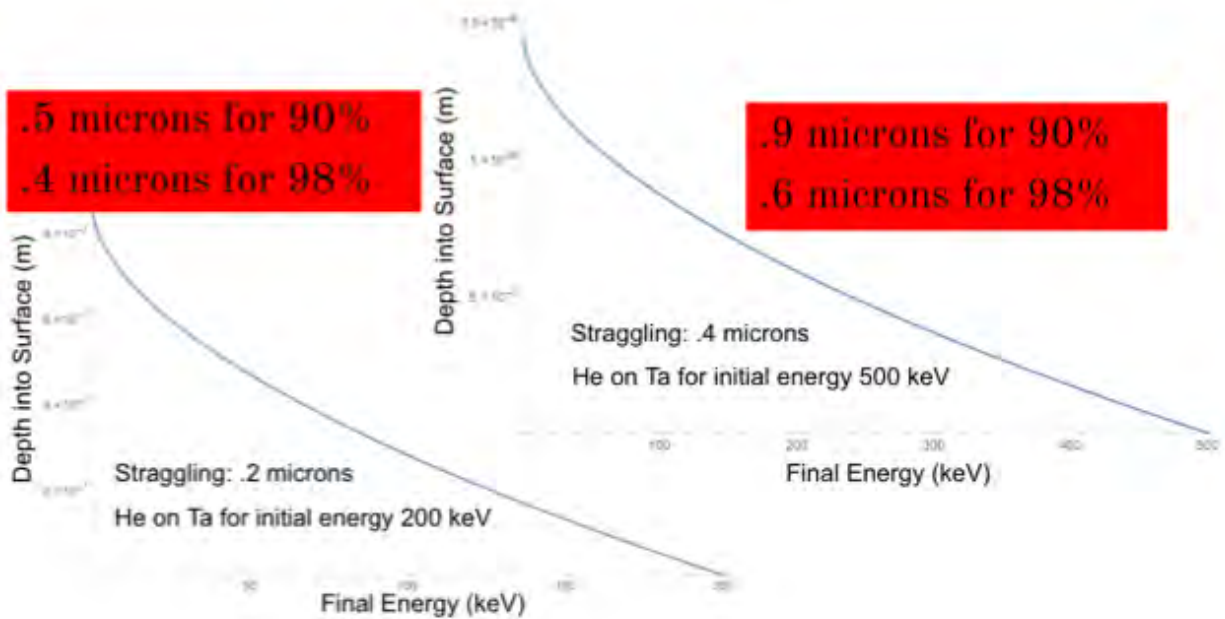


**Figure 7** - Energy of outgoing helium 4 ions as a function of the distance travelled through a tantalum surface for

**A. (left)** 200 keV.

**B. (right)** 500 keV.

The conclusion, based on a straggling of .2 microns for 200 keV particles and .4 microns for 500 keV particles, is that to get a penetration of most helium ions, the tantalum surface can be no thicker than .4-.5 microns if the ions impact with 200 keV and .6-.9 if they impact with 500 keV.

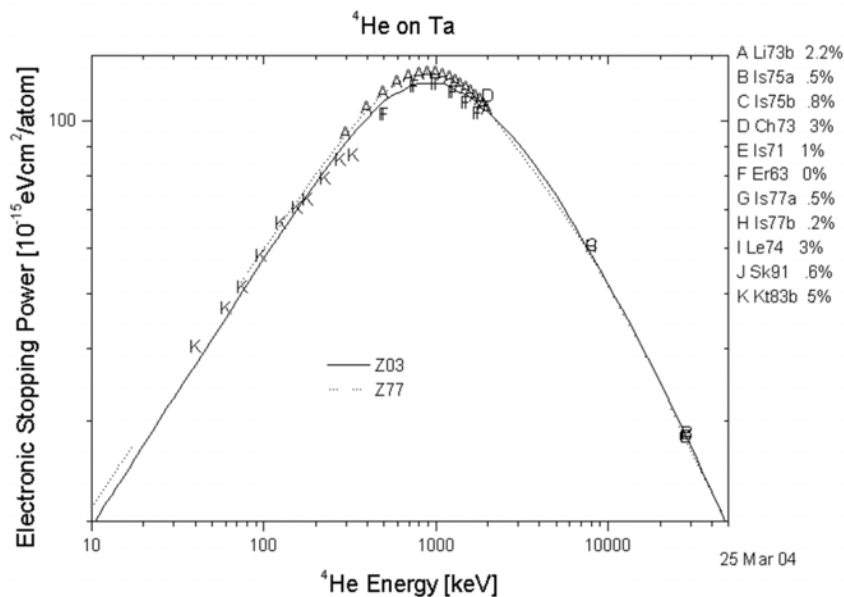


**Figure 8** - Paul's graph of stopping power versus impacting ion energy for helium 4 on tantalum as an example of what these types of graphs look like in general

Now, the experimental stopping power gives us only a mean value, i.e. out of many particles blasting through a surface it tells us the *average* stopping power. To get an idea of variation, we also need to know the "straggling," or the standard deviation of the total stopping (i.e. distance to get to 0 energy) in an experiment with data from many ions. Based on a conservative extrapolation of experimental data obtained by J.F. Ziegler, we find the straggling of helium on tantalum is about .2 microns<sup>11</sup>. This tells us that whatever maximal thickness we find is only for the *average* ion, and that the true maximal thickness is less if we want a relatively pure separation. With this in mind, we can look at Figure 7 to find that to theoretically get at least 90% of 200 keV helium ions (1.25 standard deviations) to go fully through tantalum we could be as thick as .5 microns, and to get 98% we would be looking at .4 microns. Via the same method, we find that for 500 keV helium on tantalum, where straggling is more like .4 microns (again being conservative), we get that .9 micron thickness would get us 90% through while .6 microns would get us 98%.

Based on all of this, and on the fact that most of the stopping for ions that come to a halt occurs right around the point of 0 energy, we're looking at outcoming energies of mostly between 5 keV and 100 keV. Looking at the absolute worst case of 5 keV, and based on a straggling of .03 microns from TRIM we find that our maximal thickness for a diffusion barrier is around .2 microns. While this may seem small, films of tantalum oxide can be constructed at a rate of mere nanometers per second with ion-assisted deposition<sup>12</sup>. The key point is that we predict that the tantalum cover on both sides of the tantalum oxide could allow near complete redeposition, i.e. very minimal sputtering losses. Therefore, we currently see no limit to how *thin* the tantalum oxide can be, so further studies could be done to determine the feasibility of creating a tantalum oxide layer of order of  $10^{-7}$  meters and whether it is indeed true that no

erosion or degradation occurs over long periods of time thanks to the tantalum cover. To summarize, the idea would be to deposit this thin film on a tantalum slab and then spray another tantalum layer of order of between .2 and .9 microns (depending on energy of ions and desired degree of separation) on top of that to arrive at what we see in Figure 6-A, or alternatively to get the same dimensions through oxygen implantation as described previously in this paper if it turns out to be easier to manufacture that way.

### Sputtering and Minimal Thinness

To address the *thinnest* the material can be, sputtering calculations need to be made. While the design would be largely immune from the sputtering due to deuterons (since the deuteron's energy is below the energy threshold of tantalum), the fusion products are much too energetic to ever fall below the sputtering energy threshold of any materials. Based on 200 keV helium ions, for a 1 MW power plant and a target area of 1 m<sup>2</sup>, we calculated that approximately 0.423 microns would be lost due to sputtering per week, as per the simple relation

$$\frac{\text{depth loss}}{\text{time}} = \frac{\text{fusion events}}{\text{time}} \times \frac{\text{particles}}{\text{fusion event}} \times \frac{\text{atoms lost}}{\text{particle}} \times \frac{\text{volume}}{\text{atom}} \times \frac{1}{\text{area}}$$

where

$$\frac{\text{fusion events}}{\text{time}} = \frac{\text{power}}{\text{energy release per fusion event}}$$

This would mean, if we had a surface .5 microns thick, we'd need to respray the surface with tantalum about once a week. If, however, the calculation was based on 500 keV helium ions, we would lose slightly fewer microns per week due to a lower sputtering yield and we would be able to have a higher maximal thickness (as per the discussion in the previous subsection), allowing for maintenance to be performed only every other week or even once a month. The particular energies of the exhaust species are yet to be determined in the PFRC and are within our control to some degree.

Note that Figure 6-B would contain tantalum oxide as a first surface. This surface could be thicker than the first surface of Figure 6-A since tantalum has a higher stopping power than tantalum oxide, but there's a significant issue with having tantalum oxide as the first surface: oxygen sputters much quicker than tantalum, meaning over time the tantalum oxide surface would become a degenerate, imperfect crystal consisting of much more tantalum than oxygen. This would allow fast fusion products to diffuse out either side due to a lower diffusion barrier. It would also mean that respraying would make the surface thicker and thicker over time in addition to leaving a bit of oxygen residue in the second surface that is supposed to be pure tantalum. We therefore are somewhat confident as of now that Figure 6-A is the design of choice.

### Reflection

Analyzing our design of choice, Figure 6-A, the first means of separation in surface separation (where we assume we have not been able to separate the deuterium out from the start via plasma effects) is the reflection of the deuterium ions but passage of the fusion products. For tungsten, 100 eV deuterons are reflected at a rate of 65/100, meaning 65 deuterons are reflected from the surface for every 100 ions that hit it. 100 keV fusion products, on the other hand, reflect at a rate of 4.1/100. Similarly, for tantalum, 100 eV deuterons are reflected 72/100 times, and 100 keV fusion products 3.8/100 times<sup>13</sup>. Since most of the deuterons are reflected but hardly any of the fusion products, a relatively good separation of slow deuterium from fast fusion products is achieved.

### Diffusion

The second (and final) means of separation by energy in surface separation is after the ions have been implanted (deuterons in the first surface and fast fusion products in the fast ion stopping material). This step involves the diffusion of each species in the correct direction. The diffusion coefficients are based largely on material and the temperature of that material. These diffusion coefficients, in combination with the predetermined thicknesses of each layer in Figure 6-A, can calculate the time it would take for each ion to diffuse out each side based on the following calculation:

$$\text{Diffusion Time (s)} = \frac{(\text{Thickness (m)})^2}{\text{Diffusion Coefficient } (\frac{m^2}{s})}$$

Due to difficulty determining accurate diffusion coefficients, the exact calculations for the PFRC based on thicknesses previously discusses is omitted. Further research into these diffusion coefficients is strongly encouraged.

### Separation of Fusion Products and a Cost Analysis of the Process

By cooling our fusion products to around 20 K, all hydrogen isotopes will be liquified while the helium will still be in the gas phase, so a simple distillation separates hydrogen from helium isotopes. Furthermore, through a cryogenic distillation column the hydrogen could be separated from the tritium. Note that this is where having already separated the deuterium comes in so handy - we have a binary mixture which requires fewer steps and therefore allows a much purer product at less cost. This method of separating helium from hydrogen and hydrogen isotopes from one another has already been discussed extensively, e.g. in a paper by Mikio Eoneda of the Japan Atomic Energy Research Institute<sup>14</sup>, and is based on hydrogen having a boiling point of 20.4 K while tritium is higher at 25 K<sup>15</sup>.

As for separating the helium isotopes from one another, the general idea is to cool the mixture to below the lambda point, or the temperature of 2.17 K where liquid Helium 4 becomes a superfluid. Helium 3 does not, and thanks to the characteristic near-lack of viscosity of superfluids we would easily be able to separate the two via a porous filter that does not allow liquid helium 3 through, as described in a paper by V.P. Peshkov of the Institute for Physical

Problems in the former USSR<sup>16</sup>. The idea we will be focusing on, rather than the *method* of separation, is the cost.

Based on a compilation of many sources, liquified helium 4 tanks at 4 K are currently sold at around \$5.00 per liter, which means that the worst case cost of cooling Helium to 4 K is \$5.00, since the figure also includes the overhead of the manufacturer's profit and shipping/handling costs<sup>17</sup>. Based on calculations assuming Carnot efficiency, we find that the cooling of a liter of a half and half mixture of helium 3 and 4 to 4 K would be \$0.30 and to 2.16 K would be \$0.57, using the equation

$$\text{Cooling Energy per Unit Amount} = C_v(T_f - T_i) \left( \frac{T_f - T_i}{T_f} \right)_{18}$$

and with the current cost of electricity of \$0.12 per kW-hr<sup>19</sup>. Also note that we assumed for both helium 3 and 4 a density of 35 L/mol and a constant heat capacity of 12.5 J/mol\*K<sup>20</sup> and ignored the change in heat capacity upon entering the liquid phase since that will not make a significant difference in the integral of the heat capacity since the temperature range is so small for which they are liquids (boiling point of helium 4 is 4.2 K and helium 3 is 3.2 K). Since we now know the ratio of real world to theoretical cost is \$5.00 / \$0.30 = 16.7, we can estimate that it will cost us about \$9.52 to cool a liter of a half and half mixture of helium 3 and 4.

To put this in perspective, given that fuel currently costs about \$2.13 a gallon<sup>21</sup> and stores 9.0E20 MeV<sup>22</sup> while He3 (as per the above) costs us \$9.52 / (½ liter of helium 3) = \$72.20 a gallon and stores 1.3E27 MeV (based on the D-He<sup>3</sup> reaction producing 18 MeV and the aforementioned density of liquid helium), we see that helium 3's ratio of energy content to price is 4E4 times that of fuel oil. Clearly, separation with cryogenic distillation is quite cost effective in this sense relative to just letting the exhaust stream go to waste, and this illustrates the importance of the work we have discussed throughout this paper.

## Conclusion

After analyzing several possible methods of separation, two stood out as possible candidates for a separation by energy. The design depicted in Figure 5 would separate the fast fusion products, which would barrel through the curved field, from the deuterons, who's smaller Lamar radii would have them follow the field lines. Should this fail, however, surface and volume effects could also plausibly separate the species by energy as depicted in Figure 6-A with a first surface of tantalum with thickness of .4-.9 microns and a second surface of tantalum oxide as thin as possible.

More research needs to be conducted into redeposition of the sputtered ions. Angling the surfaces in such a way that many of the sputtered atoms may recombine with the surface is one technique to overcome the sputtering problem and requires further examination. Another possible area of future consideration is the energy extraction, since that is of course fusion's essential goal. Because deuterium composes over 99% of the ions in the exhaust stream, they

carry most of the energy, despite being slower than the fusion products. Extracting this kinetic energy is crucial to the success of the PFRC.

Finally, further research into separation of the fast fusion products from one another must be conducted, but a few back of the envelope calculations tell us that cryogenic distillation could be feasible and cost-effective.

## Acknowledgements

We'd like to thank our advisors Dr. Samuel Cohen and Dr. Bruce Koel for making this research possible and all their contributions along the way. We would also like to thank their entire lab teams who helped tremendously throughout the journey.

This work was funded by Princeton Environmental Institute (PEI).

This work was supported, in part, by DOE *Contract Number DE-AC02-09CH11466*

## References

1. *System and Method for Small, Clean, Steady-State Fusion Reactors*, Docket No. Princeton 43176.
2. Strohl. "Magnetohydrodynamic Power Generator," *Encyclopedia Britannica Online*.
3. Moir, "Direct Energy Conversion in Fusion Reactors," *Lawrence Livermore Laboratories*.
4. Post, "Mirror Systems: Fuel Cycles, Loss Reduction and Energy Conversion," *Lawrence Livermore Laboratories*.
5. NRL Plasma Formulary, NRL/PU/6790--13-589, 2013, pg 28, *Naval Research Laboratory*.
6. Chen Francis, *Introduction to Plasma Physics and Controlled Fusion*, Volume 1, 2nd Edition.
7. Eubank H.P. and Wilkerson T.D., 1963, *Phys. Fluids* 6 914.
8. Schmidt George, 1960, *Phys. Fluids* 3 961.
9. Eckstein W., García-Rosales C., Roth J., and Ottenberger W. 1993 Sputtering Data *Max-Planck Institut Fur Plasmaphysik IPP 9/82*.
10. Helmut, Paul. Nuclear Data Services, Stopping Power of Matter for Ions, *International Atomic Energy Agency*, 2016.
11. Ziegler, "Range Distributions for Energetic Ions in All Elements," *IBM Research*, 1980.
12. Martin, *Properties of thin films of tantalum oxide deposited by ion-assisted deposition*, *Thin Solid Films* 238 181.
13. Ito et al. *Data on the Backscattering Coefficients of Light Ions from Solids (A Revision)*, Institute of Plasma Physics Nagoya University, June 1985.
14. Enoeda, "Hydrogen Isotope Separation Characteristics of Cryogenic Distillation Column," *Japan Atomic Energy Research Institute*, 1989.
15. Bal David, "Tritium," <http://science.jrank.org/pages/6970/Tritium.html>.
16. Peshkov V.P., 1955, *Journal of Experimental and Theoretical Physics (USSR)* 30, 850-854.
17. Elert Glenn, "Price of Liquid Helium,"

<http://hypertextbook.com/facts/2007/NadyaDillon.shtml>.

18. Alekseev, "Basics of Low-temperature Refrigeration,"  
<https://arxiv.org/pdf/1501.07392.pdf>.
19. NPR, "The Price of Electricity,"  
<http://www.npr.org/sections/money/2011/10/27/141766341/the-price-of-electricity-in-your-state>.
20. NIST Chemistry Webbook, Isobaric Properties for Helium at 1 atm.
21. AAA, Gas Costs, <http://gasprices.aaa.com/>.
22. Engineering ToolBox, "Energy Content in Common Energy Sources,"  
[http://www.engineeringtoolbox.com/energy-content-d\\_868.html](http://www.engineeringtoolbox.com/energy-content-d_868.html).